Neodymium and gadolinium extraction from molten fluorides by reduction on a reactive electrode

Christophe Nourry, Laurent Massot, Pierre Chamelot, Pierre Taxil

Neodymium and gadolinium extraction from molten fluorides by reduction on a reactive electrode

C. Nourry, L. Massot*, P. Chamelot, P. Taxil

Université de Toulouse ; INPT, UPS ; Laboratoire de Génie Chimique ; Département Procédés Electrochimiques ; F-31062 Toulouse cedex 09, France

CNRS ; Laboratoire de Génie Chimique ; F-31062 Toulouse cedex 09, France

(*) corresponding author:

Massot Laurent
Tel: + 33 (0) 5 61 55 81 94
Fax: + 33 (0) 5 61 55 61 39
E-mail: massot@chimie.ups-tlse.fr

Abstract

This work describes the electrochemical extraction on a reactive cathode (Cu, Ni) of two lanthanides Ln (Ln = Nd and Gd) from molten LiF-CaF_2 medium at 840 and 920°C for Nd and 940°C for Gd. Extraction runs have been performed and the operating conditions (cathodic material and temperature) optimised. The titration of the Nd and Gd concentrations in the melt during extraction used square wave voltammetry. At the end of each run, the residual Ln content was checked by ICP-AES; the extraction efficiencies of the two lanthanides were found to be more than 99.8% on both reactive substrates.

Key words

Fluorides, lanthanides, intermetallic compounds, electrochemical extraction, online titration.

1. Introduction

Since the 1990's, many research programs concerning molten salt reactors or nuclear fuel reprocessing propose an alternative route for the current hydrometallurgical reprocessing method. Pyrochemical methods and especially electrochemistry in molten salts have already provided promising results [1-7]. One of the key aims of the reprocessing is lanthanide extraction from the nuclear waste. Lanthanides produced during the fission reaction are highly neutrophagous and would decrease the fission reaction efficiency; furthermore, they have a relatively low radioactivity. For these reasons, they must be removed from nuclear waste, separated from the radioactive waste with a long half-life and finally extracted for storage.

The extraction could be performed in molten fluorides after dissolving the nuclear waste. The Ln are extracted in the last step, when all the other fission products have been removed from the melt.

Earlier works performed in our Laboratory have studied the electrochemical behaviour of several lanthanides in molten fluoride media [8-10]. In a previous report dedicated to the extraction of Nd and Gd from a molten fluoride mixture by electrodeposition, Nourry et al. demonstrated that:

(i) the equilibrium potential of Nd and Gd in the molten electrolyte is too close to that of solvent reduction to be able to expect complete extraction of each of the elements [11].

(ii) the use of a reactive cathode allows the reduction potential of Nd and Gd ions in alloys with the cathodic material, to be shifted towards more anodic values and consequently, the theoretical extraction efficiency to be close to 100% for these elements [11].

The present work details the implementation of the extraction process of lanthanide ions from a molten fluoride bath using a specific experimental set up as well as an online titration set up to measure the progress of lanthanide depletion from the electrolyte. The goal is to obtain, on the laboratory scale, using Cu and Ni electrodes, extraction efficiencies of higher than 99.8% in a reasonable time. The rise in temperature seems to be a good way to increase the extraction rate since it gives a liquid deposit that rapidly leaves the cathode surface avoiding saturation of the intermetallic diffusion layer which would limit the processing rate. The results are presented in such a way to allow their extrapolation to the industrial scale.

2. Experimental

- The experimental cell consisted of a vitreous carbon crucible placed in a cylindrical vessel made of refractory steel and closed by a stainless steel lid cooled inside by circulating water. The inner part of the walls was protected against fluoride vapours with a graphite liner

containing the experimental crucible. The experiments were performed under an inert argon atmosphere (U-grade: less than 5 ppm O_2), previously dehydrated and deoxygenated using a purification cartridge (Air Liquide). The cell was heated in a programmable furnace and the temperature was measured using a chromel-alumel thermocouple. A more detailed description of the device can be found in previous papers from our laboratory such as [10].

- The electrolytic bath consisted of the eutectic LiF/CaF_2 (SDS 99.99%) mixture (79/21 molar ratio). Before use, it was dehydrated by heating under vacuum (3.10^{-2} mbar) from room temperature up to its melting point (762°C) for 72 h. To provide gadolinium and neodymium ions, gadolinium fluoride GdF_3 (SDS 99.95%) and neodymium fluoride NdF_3 (SDS 99.99%) pellets were introduced into the bath through a lock chamber under argon gas atmosphere.

- Electrochemistry: for lanthanide extraction, we used the potentiostatic electrolysis mode while the titration of the elements was performed by square wave voltammetry, which we proved to be an accurate method [12;13]. Both techniques involved an Autolab PGSTAT 30 potentiostat/galvanostat controlled using the research software GPES 4.9.

- Characterisation of reduction products: after electrolysis, the cathode surface was examined by scanning electron microscopy (LEO 435 VP) equipped with an EDS probe (Oxford INCA 200) for determining the composition of the alloys. Inductively coupled plasma – atomic emission spectroscopy (ICP – AES Jobin-Yvon JY24) was used for Nd(III) and Gd(III) content determination after sampling the melt.

- *(I) Analytical set-up*

For investigations concerning the electrochemical behaviour of the fluoride bath used for the subsequent extractions, the following cell was used:

Mo (1 mm diameter), Ni (1 mm diameter) or Cu (1.2 mm diameter) were used as working electrode; the surface area of the working electrode was determined by measuring its

immersion depth in the bath after withdrawal from the cell; the auxiliary electrode was a vitreous carbon rod (3 mm diameter) with a large surface area. Potentials were referred to a platinum wire (0.5 mm diameter) immersed in the molten electrolyte, acting as a quasi-reference electrode $Pt/PtO_x/O^{2-}$ [14].

- *(II) Extraction set-up*

Compared with the previous set-up, the extraction device needed specific arrangements, because of the consequences of long-term experiments causing both significant changes in the electrolyte composition and the production of unacceptable gases at the anode (anode effect), as detailed below:

(i) the quantitative extraction from the bath of Ln elements promotes a change of free oxide content in the melt, as we know that Ln fluoride reacts with oxide ions to form Ln oxifluoride [15], and that the release of Ln from the bath changes the free oxide content in the bath, making the use of the platinum quasi-reference electrode unreliable. Consequently, we must use a reference electrode insulated from the electrolytic bath: it was a 1-mm diameter nickel wire immersed in a mixture of $LiF\text{-}CaF_2\text{-}NiF_2$ (1 mass %), placed in a boron nitride basket. This reference electrode was proved to be reliable in molten fluoride baths [16]. Moreover, the insulation from the electrolytic bath guarantees the invariability of its potential with the change of composition of the electrolyte.

(ii) the vitreous carbon anode was isolated in a graphite compartment containing a $LiCl\text{-}LiF\text{-}CaF_2$ eutectic mixture. The anodic reaction was chlorine release instead of CF_x formation; besides, electrode compartmentalisation avoided gas release in the cell atmosphere and the possibility of reoxidation of Ln-M compounds formed at the cathode.

(iii) the working electrodes were copper and nickel plates with a large surface area (4 cm^2).

3. Results and discussion

3.1. Previous results obtained on the electrochemical behaviour of Nd(III) and Gd(III) on reactive electrodes

Reference [11] dealt with our results on the electrochemical behaviour of Nd(III) and Gd(III) on reactive nickel and copper electrodes. The work showed that Nd(III) and Gd(III) could be reduced by alloying with the cathodic material (Cu or Ni) at far more anodic potentials than on an inert cathode; this so called "depolarization effect", allows the theoretical extraction efficiency of these lanthanides to be enhanced up to 100%.

Concerning the titration of Ln ions during electrolysis, previous works in our laboratory, showed that square wave voltammetry (SWV) is a suitable technique to monitor the electroactive species content of molten fluoride media [17;18]. Consequently, as the lanthanide ion concentration decreases during extraction runs, SWV can be used to check the Nd(III) and Gd(III) contents without sampling the molten solution.

Figures 1 and 2, which compare the SW voltammograms plotted at 840°C, on inert (Mo) and reactive (Ni, Cu) cathodes, for LiF-CaF_2-NdF_3 and LiF-CaF_2-GdF_3 systems respectively, indicate the occurrence of depolarization. These curves were plotted for several Nd(III) and Gd(III) concentrations in order to establish calibration curves ($\delta i_p = f(C)$), for each system, reported in Figures 3 and 4. It can be noted that, for both Nd and Gd, these calibration curves are composed of two parts depending on the lanthanide concentration: for contents higher than around 3 10^{-3} mol kg^{-1} (area I), or lower (area II). A Mo electrode can be used for SWV lanthanide titration at high Ln concentrations whereas for low contents, Ni or Cu electrodes must be used, since in this part no cathodic current is detectable on the Mo electrode.

In order to validate this titration method, the results from SWV titration were compared with ICP analyses after sampling four times during the extraction and once after. Good agreements between the respective results validated our online methodology of Ln titration.

3.2 Extraction experimental procedure

The volume of the electrolytic bath was $V_{sol} = 100\ cm^3$.

Two kinds of working electrodes were introduced in the electrolyte:

(i) cathode for extraction (CE): it is a plate with a large surface area ($S_{el} = 4\ cm^2$). Note that the kinetics vary linearly with the ratio S_{el}/V_{sol} and thus all the following results can be extrapolated to a larger scale.

(ii) Working electrode for titration of remaining Ln in the bath (TWE) which was a Cu or Ni wire immersed in the bath.

The experimental set-up is described in the experimental part (§ 2) with a specific reference electrode and an anodic compartment. The use of a reference electrode insulated from the electrolytic bath insures the stability of the potential reference adapted to long-term potentiostatic electrolysis runs, as explained above. So, in the electrolysis part of the article, potentials are referred to the NiF_2/Ni electrode system.

Electrolyses were performed in potentiostatic mode and the experimental procedure was the following:

(i) recording a SW voltammogram on a TWE to determine the electrolysis potential; we took the potential of the alloying reduction peak presented in Figures 1 and 2. As reported in ref [11], the voltammogram peaks correspond to the formation of Ni_5Nd, Cu_6Nd, Ni_5Gd and Cu_6Gd respectively.

(ii) introduction of a EC into the bath for an electrolysis time of around 3 hours to recover the alloy; this electrode was then removed from the experimental medium.

(iii) recording a SW voltammogram on a TWE to measure the level of Ln ions remaining in the bath and, accordingly, the progress of the extraction process.

(iv) these three stages were repeated as a long as any electrochemical signal was detected by SW voltammetry.

3.3 Neodymium extraction on copper and nickel

3.3.1 Extraction at T = 840°C

Extraction experiments were performed on CE at T = 840°C. As mentioned above, the process was followed by periodically plotting SW voltammograms of the solution. Typical SW voltammograms obtained on a Cu (TWE), at increasing extraction durations (t = 0; 2.5; 15 and 45 h), are presented in Figure 5. A significant decrease of the current density is observed on the SWV. It is correlated with the decrease of the Nd(III) ion concentration in the bath during the extraction process. We noticed that the current density decreased more rapidly at the beginning of electrolysis than after longer times, suggesting an exponential decrease of [Ln(III)] versus time. Similar experiments were carried out on a nickel electrode at the same temperature.

3.3.2 Extraction efficiency and normalized time

From the calibration curves presented above for Nd(III) reduction on a Mo, Cu or Ni electrode, the measurement of the cathodic peak current density allowed the remaining Nd(III) ion concentration in the melt, and consequently the extraction efficiency η, to be calculated. η is expressed as below:

$\eta = \frac{C_i - C_f}{C_i}$ where C_i and C_f are the initial and final Nd(III) concentrations respectively.

As mentioned above, we assumed that the kinetics is linear with the S_{el}/V_{sol} ratio, which leads us to define a so-called "normalized time" $t^* = t\ (S_{el}/V_{sol})$, as the time variable of the process.

Hence, the variation of the extraction efficiency η was plotted versus the normalised extraction time in Figure 6 for Cu and Ni electrodes. No significant difference can be observed at 840°C between extraction on Cu and Ni electrodes; the bath was sampled at the end of the extraction process, and from the ICP-AES titration results, the extraction efficiency was determined to be 99.8% in neodymium for both Cu and Ni electrodes. However, the final electrolysis times, to reach a cathodic current density approaching zero, are slightly different: 1.8 h cm^{-1} and 1.6 h cm^{-1} for Cu and Ni respectively.

The inset in Fig. 6, showing the linear relationship between $\ln(1/(1-\eta))$ and the normalized time for the Ni electrode, confirms the exponential form of the Ln content decrease, which can be expressed as:

$$[Ln(III)] = [Ln(III)]^{\circ} \exp(-K\, t^*) \qquad (1)$$

where K is a kinetic parameter depending on the rate of both the intermetallic surface reaction and solid diffusion.

3.3.3 Influence of the operating temperature on the extraction duration

Naturally, the kinetic constant must be influenced by the temperature and the physical state (solid or liquid) of the cathodic product.

To examine the temperature effect, several extractions were performed on Ni and Cu electrodes at 920°C, using the same procedure as above. The results are compared with those obtained above at 840°C in Figures 7 (Ni) and 8 (Cu).

(i) Figure 7 does not show a significant difference in the "in situ" measurements of Nd extraction efficiency; nevertheless the normalized time of complete extraction at 920°C was 1.4 h cm^{-1} instead of 1.6 h cm^{-1} at 840°C. This slight difference is only due to the increase of the kinetic constant K with the temperature; note that the binary phase diagram indicates that none of the Ni-Nd alloys are liquid at 920°C [19].

(ii) In contrast, the Cu-Nd binary diagram [19] predicts the formation of liquid compounds at 920°C. Accordingly, the kinetic process must be enhanced by the continuous removal of product from the cathode surface which is therefore continuously renewed, avoiding the kinetic limitations of intermetallic diffusion. This assumption is verified in Figure 8 where we observe a rapid decrease of the Ln content at 920°C compared to 840°C. The same final extraction efficiency was obtained in 0.4 h cm^{-1} at 920°C instead of 1.8 h cm^{-1} at 840°C; this represents a decrease of more than four-fold over the whole duration of reprocessing.

Compared with the case when nickel is used as reactive cathode, such a large decrease in reprocessing duration with a small increase in temperature is attributed to the liquid state of the cathodic Cu/Nd product continuously leaving the electrode surface and hence, avoiding saturation of the solid diffusion layer. This result confirms that in the overall reaction process, the limiting step is intermetallic diffusion.

After extraction, cross-sections of the Cu cathodes were observed by SEM (see Figure 9). The structure of the intermetallic layer is typical of a eutectic mixture formed during the electrode cooling stage. This assumption can be verified by examining the Cu-Nd binary phase diagram [19] presented in Figure 10. At 920°C, the composition of the liquid phase produced was 7 atom % Nd. Then, during the cooling stage, this phase decomposed into Cu

and Cu_6Nd, as observed in Figure 9, with a global level of Nd in the diffusion layer of 9 atom %.

3.4 Gadolinium extraction

As the binary phase diagram of Cu-Gd [19] is quite similar to that of Cu-Nd, the optimised operating conditions described above for Nd extraction (Cu electrode) were used for Gd extraction. As for Nd extraction, the temperature chosen (940°C) was propitious the formation of a liquid phase at the copper cathode during the extraction electrolysis.

Figure 11 presents the variation of the SW voltammograms of the LiF-CaF_2-GdF_3 system at 940°C on a copper electrode for different electrolysis times. A rapid decrease of the electrochemical signal can be observed up to the complete disappearance of the Gd(III) reduction peak. Using the calibration curves in Figure 4, the extraction efficiency of Gd is plotted versus the normalised time in Figure 12. This graph is comparable to that of Fig. 8 for Nd extraction on copper and the final extraction efficiency obtained in 0.4 h cm^{-1} was measured by ICP-AES to be at least 99.8%.

So, the results confirm that both gadolinium and neodymium can be completely extracted in a reasonable time from molten fluoride baths.

4. Conclusion

Removal of Nd(III) and Gd(III) from molten LiF-CaF_2 was performed by electrochemical reduction on copper and nickel electrodes. The main conclusions drawn from our results are that:

(i) the variation of the extraction efficiency obeys an exponential law with the so-called normalized time $t^* = t\ (S_{el}/V_{sol})$. Accordingly, the results obtained here can be extrapolated to other scales.

(ii) the complete extraction of lanthanides can be achieved with a reasonable processing time.

(iii) the kinetic process is considerably speeded up by the formation of liquid cathodic products. Therefore, the cathodic material and the temperature are critical parameters. In the present work, copper as cathode material and the temperature of 920°C multiplied the extraction rate more than four-fold, compared to that obtained with Ni at 920°C, or at 840°C, with either Cu or Ni,. These results highlight the great relevance of intermetallic diffusion in the overall mechanism of extraction of Ln elements using a reactive cathode material.

References

[1] Sakamura Y, Hijikata T, Kinoshita K, Inoue T, Storvick T S, Krueger C L, Grantham L F, Fusselman S P, Grimmett D L, Roy J J (2000) J Nucl Sci Technol 35:49

[2] Serp J, Allibert M, Le Terrier A, Malmbeck R, Ougier M, Rebizant J, Glatz J P (2005) J Electrochem Soc 152:C167

[3] Cassayre L, Malbeck R, Masset P, Rebizant J, Serp J, Soucek P, Glatz J P (2007) J Nucl Mat 350:49

[4] Serp J, Lefebvre P, Malmbeck R, Rebizant J, Vallet P, Glatz J P (2005) J Nucl Mat 340:266

[5] Conocar O, Douyere N, Glatz J P, Lacquement J, Malmbeck R, Serp J (2006) Nucl Sci Eng 153:253

[6] Kinoshita K., Kurata M, Inoue T (2000) J Nucl Sci Technol 37:75

[7] Taxil P, Cassayre L, Chamelot P, Gibilaro M, Massot L, Nourry C (2009) J Fluorine Chem 130:94

[8] Hamel C, Chamelot P, Taxil P (2004) Electrochim Acta 49:4467

[9] Nourry C, Massot L, Chamelot P, Taxil P (2008) Electrochim Acta 53:2650

[10] Massot L, Chamelot P, Taxil P (2005) Electrochim Acta 50:5510

[11] Nourry C, Massot L, Chamelot P, Taxil P (2009) J. App. Electrochem DOI: 10.1007/s10800-008-9740-y.

[12] Chamelot P, Lafage B, Taxil P (1997) Electrochim Acta 43:607

[13] Massot L, Cassayre L, Chamelot P, Taxil P (2007) J Electroanal Chem 606:17

[14] Berghoute Y, Salmi A, Lantelme F (1994) J Electroanal Chem 365:171

[15] Taxil P, Massot L, Nourry C, Gibilaro M, Chamelot P, Cassayre L (2009) J Fluorine Chem 130:94

[16] Taxil P, Qiao Z (1985) J Chem Phys 82:83

[17] Chamelot P, Lafage B, Taxil P (1994) Electrochim Acta 39:2571

[18] Massot L, Chamelot P, Bouyer F, Taxil P (2003) Electrochim Acta 48:465

[19] Binary Alloy Phase Diagrams (1996) 2nd Edition. ASM International, Materials Park

Legend of Figures

Figure 1:

Square Wave Voltammograms of LiF-CaF_2-NdF_3 (1.5 10^{-2} mol kg^{-1}) system at 840°C on molybdenum, nickel and copper electrodes; f = 9 Hz; Aux. El.: vitreous carbon; Ref. El.: Pt

Figure 2:

Square Wave Voltammograms of LiF-CaF_2-GdF_3 (1.7 10^{-2} mol kg^{-1}) system at 840°C on molybdenum and copper electrodes; f = 9 Hz; Aux. El.: vitreous carbon; Ref. El.: Pt

Figure 3:

Calibration curves for Nd(III) titration on Mo, Ni and Cu electrodes obtained by square wave voltammetry at 840°C and 9 Hz.

Figure 4:

Calibration curves for Gd(III) titration on Mo and Cu electrodes obtained by square wave voltammetry at 840°C and 9 Hz.

Figure 5:

Square wave voltammograms plotted after different electrolysis durations in the LiF-CaF_2-NdF_3 system at 840°C; f = 9 Hz; Working El.: Cu, Aux. El.: vitreous carbon, Ref. El.: Ni(II)/Ni.

Figure 6:

Variation of the extraction efficiency of Nd at 840°C on copper and nickel electrodes versus t*, the normalized electrolysis time.

Inset: Linear relationship between $Ln(1/(1-\eta))$ and t* for Nd extraction on nickel at 840°C.

Figure 7:

Variation of the extraction efficiency of Nd on nickel electrode at 840°C and 920°C versus the normalized electrolysis time.

Figure 8:

Variation of the extraction efficiency of Nd on copper at 840°C and 920°C versus the normalized electrolysis time.

Figure 9:

SEM micrograph of a copper electrode used for the extraction electrolysis at 920°C.

Figure 10:

Cu-Nd phase diagram [16]. Cooling path of the Cu/Cu_6Nd eutectic

Figure 11:

Square wave voltammograms plotted after different electrolysis durations in the $LiF-CaF_2-GdF_3$ system at 920°C, 9 Hz; Working electrode: Cu, Aux. El.: vitreous carbon, Ref. El.: Ni(II)/Ni.

Figure 12:

Variation of the extraction efficiency of Gd at 940°C on copper electrode versus normalized electrolysis time.

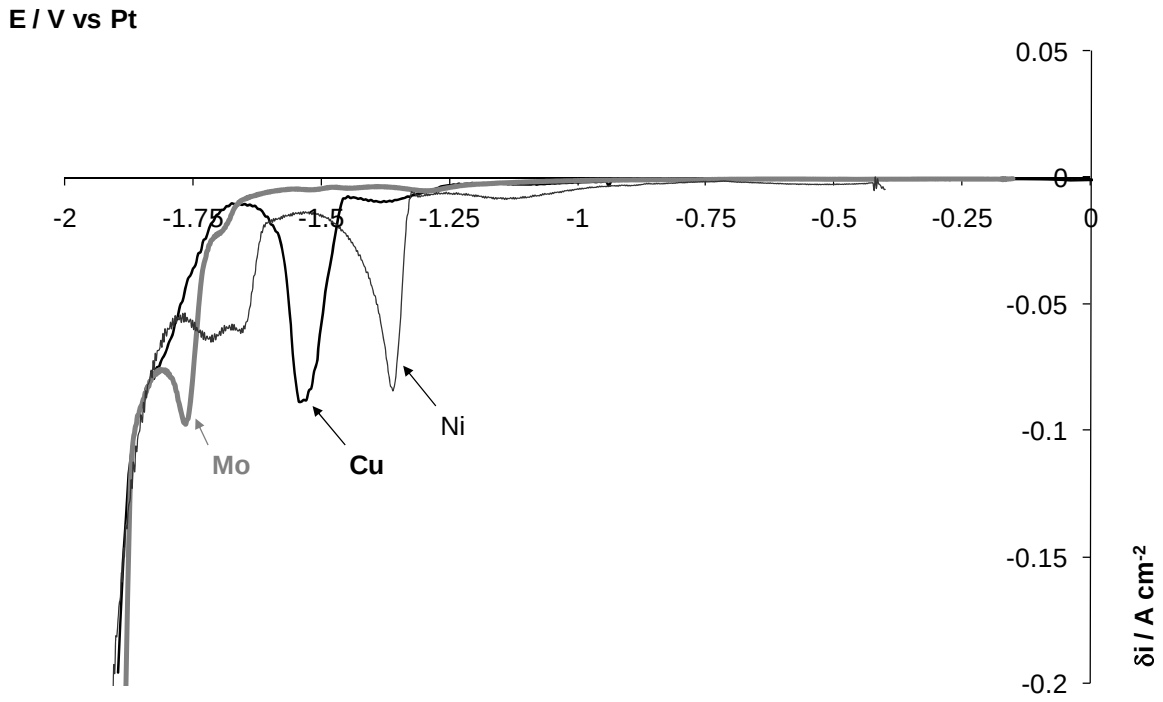

Figure 1

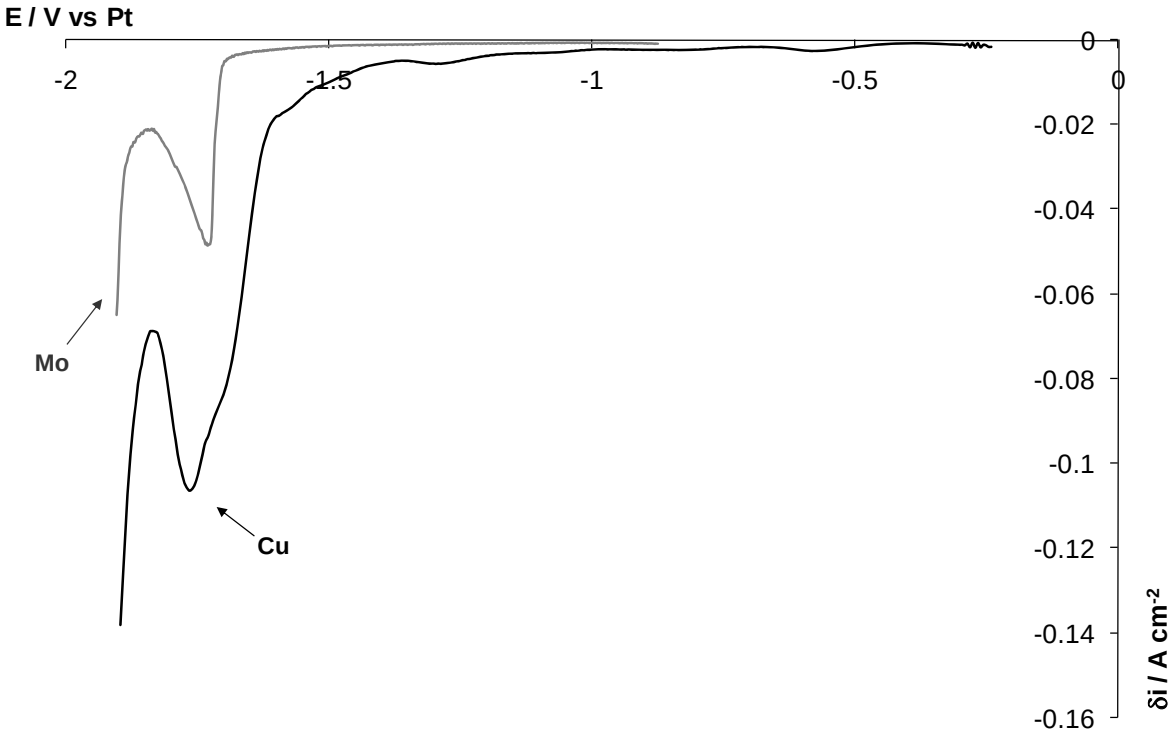

Figure 2

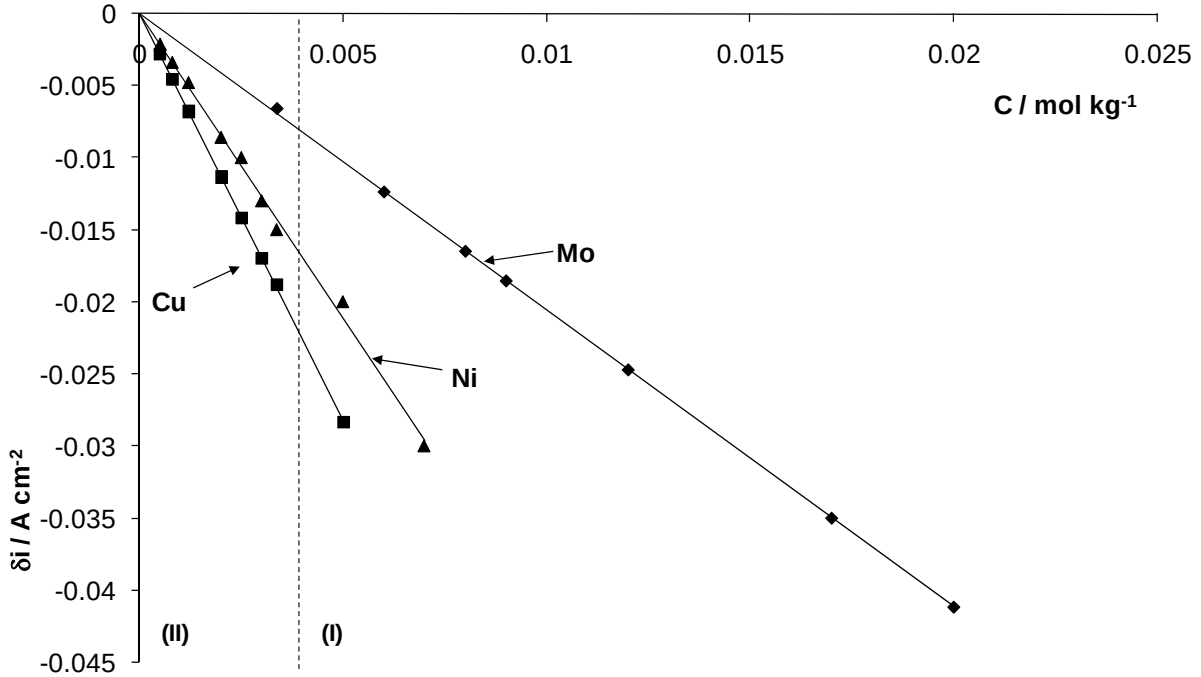

Figure 3

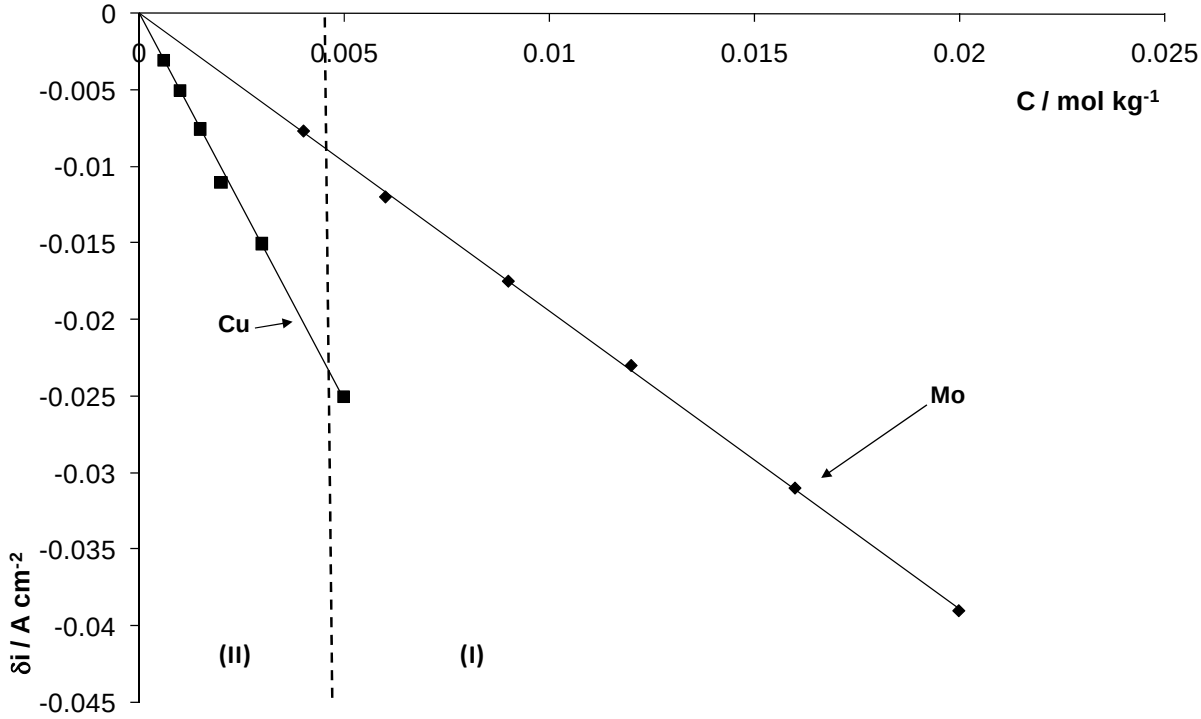

Figure 4

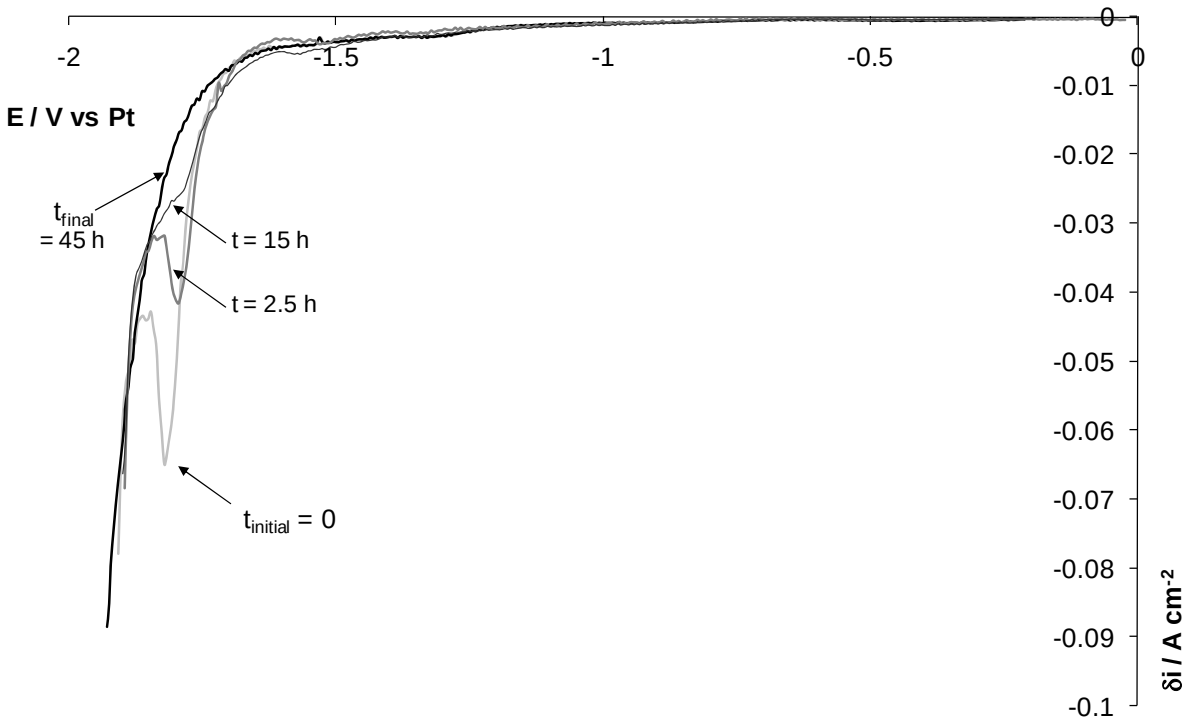

Figure 5

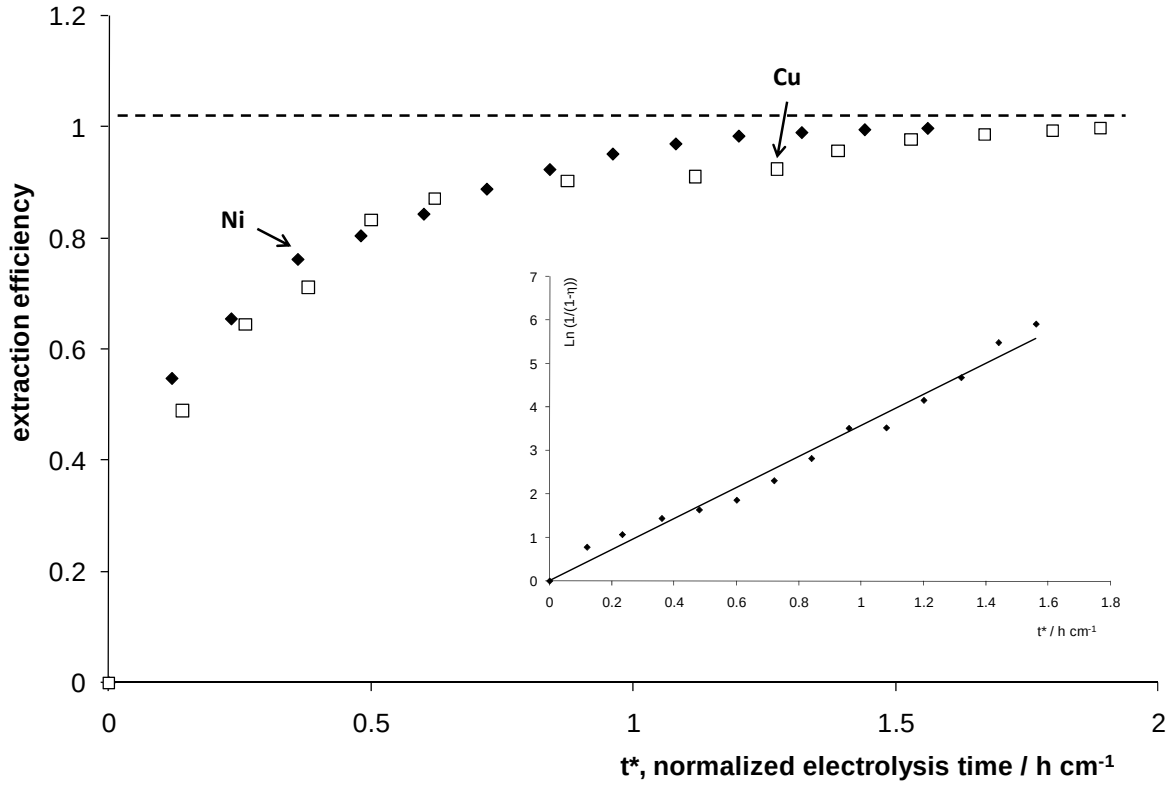

Figure 6

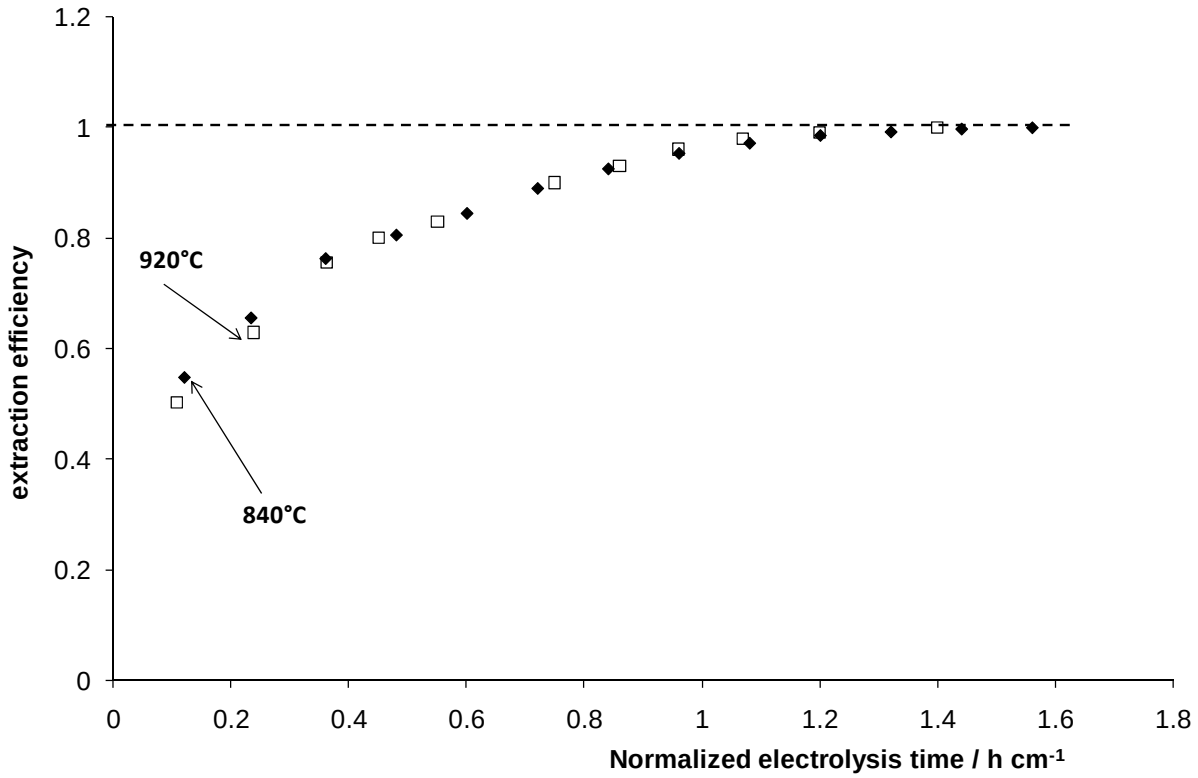

Figure 7

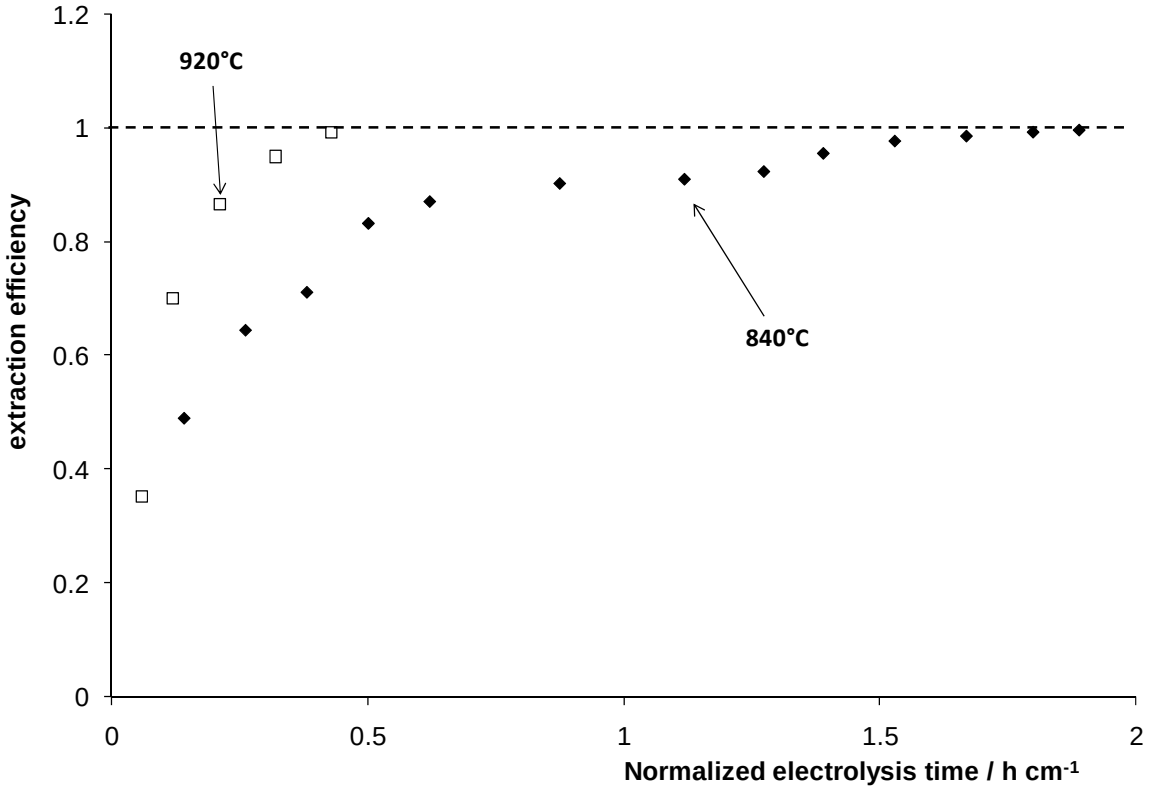

Figure 8

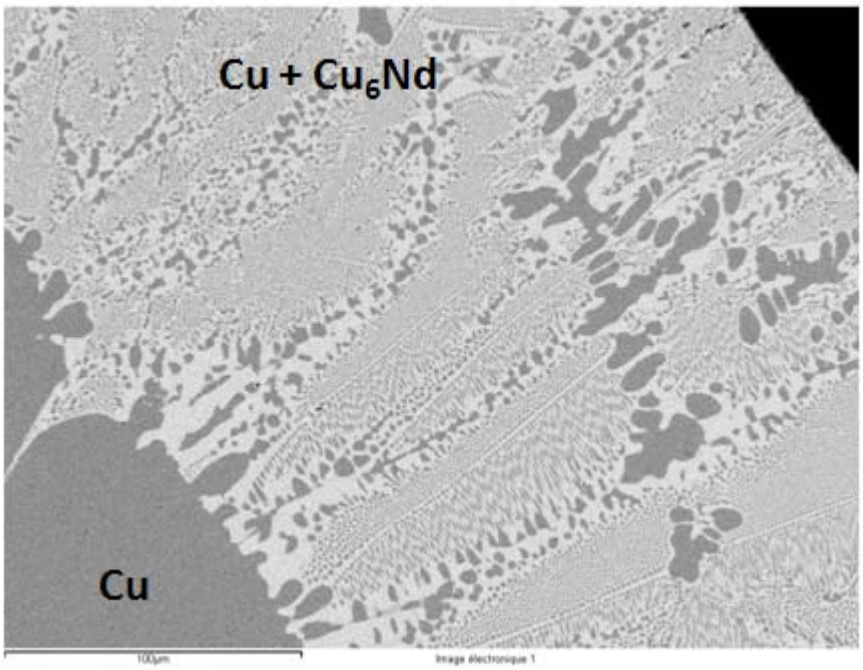

Figure 9

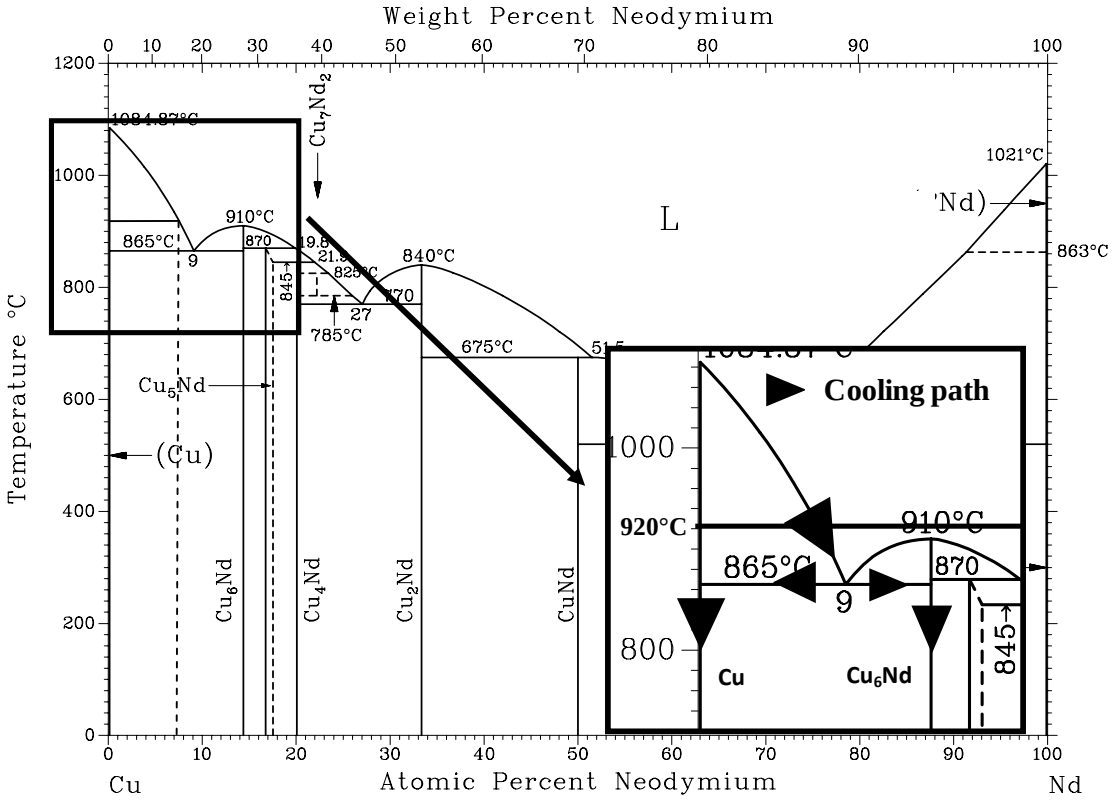

Figure 10

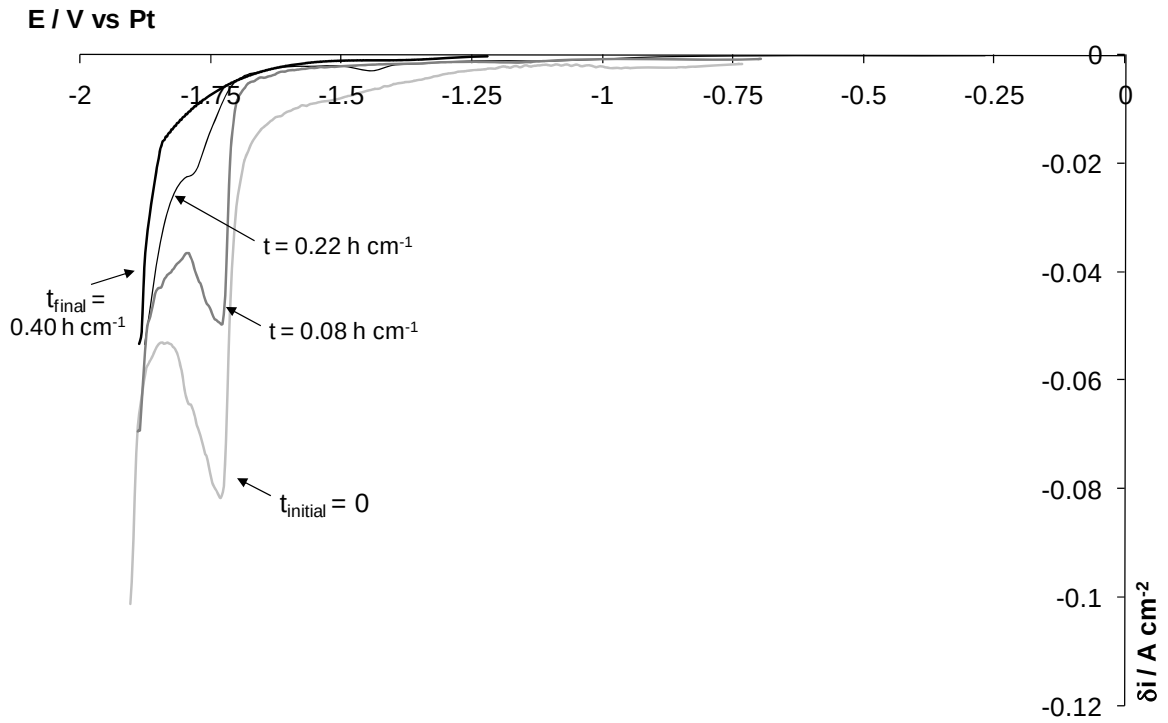

Figure 11

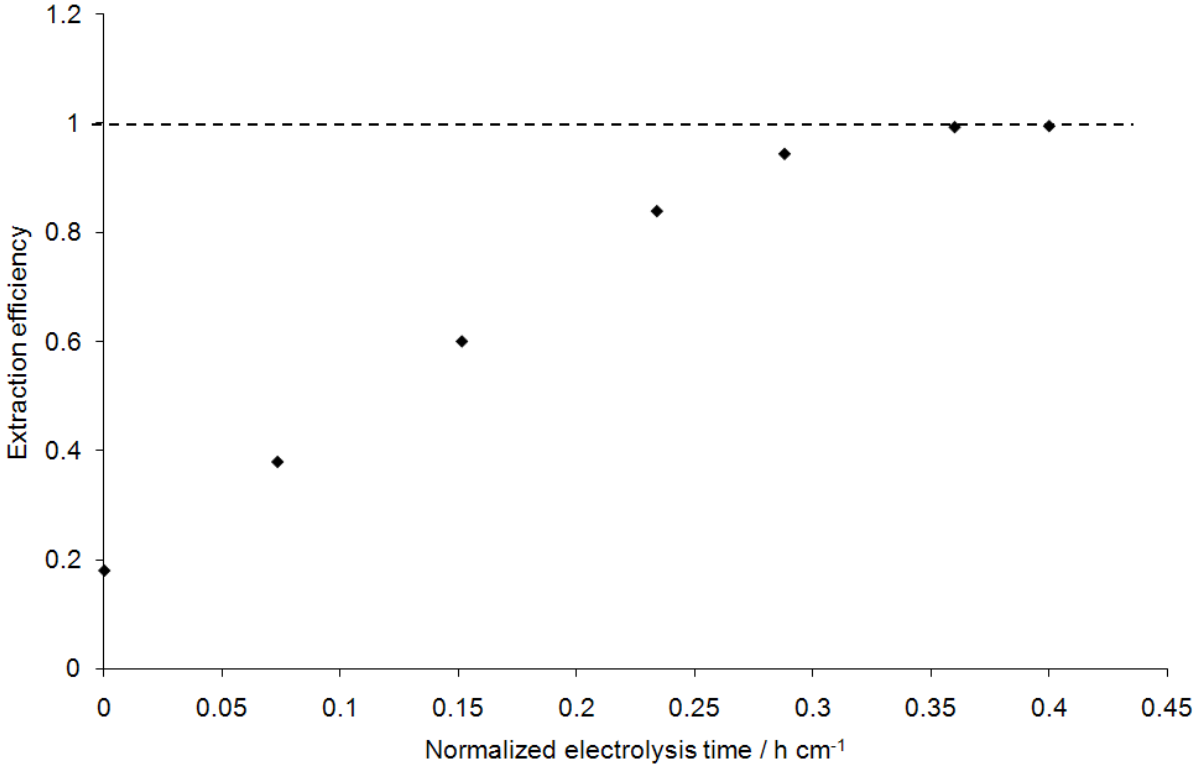

Figure 12